

ViT-FIQA: Assessing Face Image Quality using Vision Transformers

Andrea Atzori¹ Fadi Boutros¹ Naser Damer^{1,2}

¹Fraunhofer Institute for Computer Graphics Research IGD, Darmstadt, Germany

²Department of Computer Science, TU Darmstadt, Germany

andrea.atzori@igd-extern.fraunhofer.de, {fadi.boutros, naser.damer}@igd.fraunhofer.de

Abstract

Face Image Quality Assessment (FIQA) aims to predict the utility of a face image for face recognition (FR) systems. State-of-the-art FIQA methods mainly rely on convolutional neural networks (CNNs), leaving the potential of Vision Transformer (ViT) architectures underexplored. This work proposes ViT-FIQA, a novel approach that extends standard ViT backbones, originally optimized for FR, through a learnable quality token designed to predict a scalar utility score for any given face image. The learnable quality token is concatenated with the standard image patch tokens, and the whole sequence is processed via global self-attention by the ViT encoders to aggregate contextual information across all patches. At the output of the backbone, ViT-FIQA branches into two heads: (1) the patch tokens are passed through a fully connected layer to learn discriminative face representations via a margin-penalty softmax loss, and (2) the quality token is fed into a regression head to learn to predict the face sample’s utility. Extensive experiments on challenging benchmarks and several FR models, including both CNN- and ViT-based architectures, demonstrate that ViT-FIQA consistently achieves top-tier performance. These results underscore the effectiveness of transformer-based architectures in modeling face image utility and highlight the potential of ViTs as a scalable foundation for future FIQA research <https://cutt.ly/irH1zXUC>.

1. Introduction

FIQA estimates the utility value of a face sample for FR [22]. These algorithms analyze a face image to generate a scalar quality score - namely the Face Image Quality (FIQ) score - to quantitatively measure the face image’s suitability for use in FR systems [16]. High FIQA scores suggest better sample recognisability, thus increasing FR efficiency in applications such as automated border control [16, 39]. FIQA focuses on evaluating the utility of a face image for automated FR [16, 22, 39], and does not aim to measure (nor reflect) the perceived image quality. The perceived image

quality has been explored through general image quality assessment (IQA) methods [29, 32, 33], which offer insights into image quality from the perspective of human perception. However, IQA does not necessarily correlate with the face image’s utility for FR [14]. For example, a face image might score high on perceived quality according to IQA metrics but still be less suitable for FR due to issues like occlusion or extreme pose [45]. Conversely, FIQAs provide a focused evaluation of the image’s utility for FR tasks. Thus, as noted in [1, 7, 31, 36], FIQA methods in literature demonstrate superiority over IQA when assessing the utility of a face image for FR.

This paper proposes ViT-FIQA, a novel approach that extends ViTs to predict FIQ. We achieved that by extending the standard ViT designed for FR with a dedicated learnable token that attends to all image patches and learns to regress a scalar quality score. The quality token is processed as an image token with a position encoding of zero and initialized as a learnable embedding. Then, it is added to the sequence of patch embeddings at the input of the transformer. At each transformer layer, it attends to all the image patches via self-attention, gathering global, contextual information about the whole face image. This final representation of the quality token is passed through a regression layer to output a scalar quality score. This regression layer is optimized using CR-FIQA loss [7], which quantifies the relative classifiability of a sample as the ratio between the similarity to its class center and that of its closest negative class. This integration ensures that the predicted quality score aligns with the underlying FR task, maintaining tight coupling between the quality assessment and the recognition pipeline. We conducted extensive evaluations of ViT-FIQA across diverse benchmarks (LFW, CA-LFW, AgeDB-30, Adience, XQLFW, CFP-FP, CP-LFW), under cross-model FR evaluation setups using both CNN-based and ViT-based FR models. Our results show that ViT-FIQA consistently ranks among top-performing methods, particularly excelling in pose- and quality-challenging datasets. By exploring the synergy between ViTs and FIQA, our work offers new insights into using ViT for modeling face image

utility, advancing the SOTA in several experimental setups.

2. Related Work

ViTs in Face Recognition: ViTs [11] have emerged as powerful competitors to CNNs, achieving comparable performance on various vision tasks, including segmentation [26] and detection [49] despite lacking convolutional inductive biases. Early attempts to apply ViTs to FR demonstrated the viability of transformer-based architectures in this domain. FaceTransformer [53] adopted pure-transformer backbones and achieved competitive accuracy on verification benchmarks. ClusFormer [35] introduced an unsupervised transformer-driven approach for clustering faces at a large scale, outperforming previous unsupervised clustering methods in FR tasks. Part-fViT [43] introduced a ViT-based FR pipeline in two stages. First, a fViT backbone is proposed as a baseline, trained with a standard margin-based loss. Second, a part-based ViT is used to learn to predict facial landmark locations without the need for ground-truths, in order to feed the patches extracted in the predicted locations to the fViT. TransFace [9] introduced DPAP (Dominant Patch Amplitude Perturbation), a patch-level augmentation that perturbs dominant patch pixels to increase data diversity without losing facial structure, and EHSM (Entropy-based Hard Sample Mining), which uses token entropy to weight easy vs. hard samples during training. S-ViT [24] proposed a sparse vision transformer pruned for FR efficiency, which prunes redundant attention heads and tokens during training to reduce model size without sacrificing accuracy. KP-RPE [25] introduced a method to make ViT models more robust to misalignment and pose variations in face images by leveraging facial landmarks in the positional encodings. Since Relative Position Encoding (RPE) biases ViT attention toward nearby patches, the proposed KP-RPE anchors the positional importance relative to landmark locations (e.g. eyes, nose) rather than just patch distance, achieving marked improvements in accuracy when face alignment fails or faces undergo affine transformations, enhancing robustness to occlusions and pose changes.

Face Image Quality Assessment: Existing FIQA approaches fall into four groups. (1) Label-generation approaches [4, 19, 36] train regression networks using quality labels from human assessments [4], ICAO-compliance comparisons [19], or distribution distances [36]. RankIQ [8] adopts a learning-to-rank strategy, predicting quality rankings based on FR performance across datasets to better capture relative differences. These methods often rely on separate, shallow models, limiting their ability to exploit high-capacity FR features. (2) Non-FR model approaches include DiffFIQA [2], which leverages diffusion models to assess embedding robustness, and eDiffFIQA [3], which distills this into a lighter model for faster inference. These

approaches can be accurate but are typically computationally expensive due to reliance on large generative models [2]. (3) Pre-trained FR analysis approaches operate directly on a fixed FR model. SER-FIQ [44] measures embedding stability under dropout perturbations, while GraFIQ [28] uses gradient magnitudes to evaluate alignment with the FR model. FaceQAN [54] estimates quality by quantifying adversarial robustness: higher-quality images require larger perturbations to reduce recognition confidence. These methods avoid training but are constrained by the fixed FR backbone. (4) FR-integrated approaches embed quality directly into the FR process. MagFace [31] links quality to embedding magnitude via regularized training, while PFE [42] models embeddings as Gaussians with uncertainty representing quality. CR-FIQA [7] estimates quality by predicting a sample’s relative classifiability. These methods leverage the full expressiveness of the FR model and achieve SOTA performance on key benchmarks [47].

Despite recent advancements in FIQA, especially in the approaches in the fourth group, and in the utilization of ViTs for FR, the FIQ concept within ViT-based FR was never explored. To address this, we propose a novel FIQA solution that modifies a standard ViT architecture to learn a regression problem to estimate the FIQ score during FR training by (1) using a dedicated trainable token aimed to capture sample utility insights via self-attention and (2) using the original ViT backbone to produce a unique representation for both FR training and FIQ regression, as in [7].

3. Methodology

This section presents our FIQA approach that leverages a learnable quality token to capture, through the sequence of attention layers composing the ViTs, discriminant information about the classifiability (utility) of face sample. We provide first details about the ViT architecture followed by our ViT-FIQA.

ViT: ViTs [11] adapt the Transformer architecture, originally designed for NLP, to vision tasks. Unlike CNNs, which exploit local receptive fields and translation-invariant filters, ViTs use global self-attention to model long-range dependencies between image regions.

Patch Embedding: Given an input image $\mathbf{x} \in \mathbb{R}^{H \times W \times C}$, we partition it into N non-overlapping patches of size $P \times P$. Each patch is flattened and linearly projected into a D -dimensional embedding space, yielding:

$$\{\mathbf{e}_1, \mathbf{e}_2, \dots, \mathbf{e}_N\}, \quad \mathbf{e}_i \in \mathbb{R}^D.$$

Positional embeddings $\{\mathbf{p}_1, \dots, \mathbf{p}_N\}$ are added to retain spatial structure:

$$\mathbf{z}_i^{(0)} = \mathbf{e}_i + \mathbf{p}_i.$$

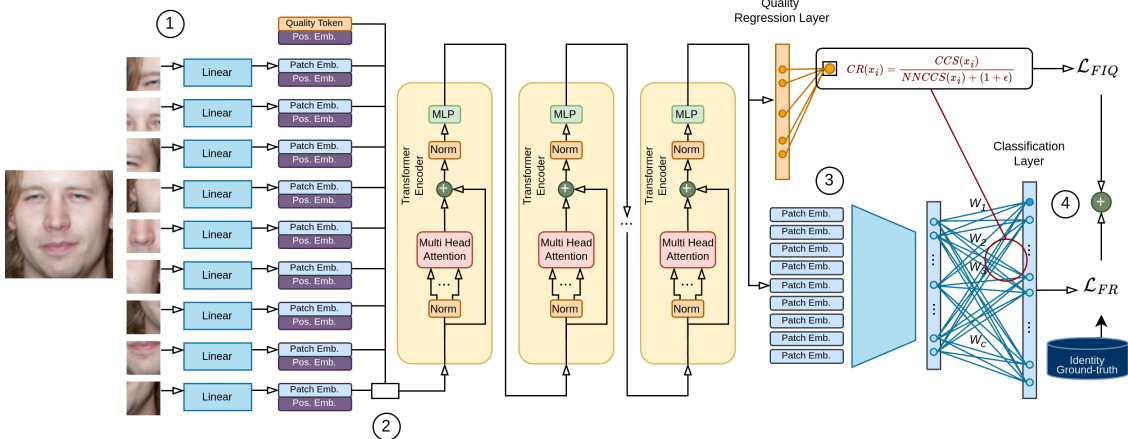


Figure 1. Overview of our ViT-FIQA. 1) A face sample is divided in equally sized, non-overlapping patches of size $P \times P$. All these patches are then flattened and linearly projected to extract the embeddings. 2) A learnable quality token is concatenated to the patch tokens. The concatenated tokens are fed as input to a sequence of Transformer Encoder layers. 3) The final sequence of embeddings is then used as follows: the first one - the refined quality token - is used as input to the regression layer in order to predict the utility value of the sample, while the remaining patches are used as input for a fully connected layer to obtain a final embedding representing the sample. 4) The two loss terms (L_{FR} and L_{FIQ}) are computed and added to obtain the final loss value.

Incorporating the Quality Token: In ViT-FIQA, we introduce an additional *learnable quality token* \mathbf{q}_0 designed to regress a scalar face image utility score. The input sequence becomes:

$$\mathbf{Z}^{(0)} = [\mathbf{q}_0 + \mathbf{p}_0; \mathbf{z}_1^{(0)}, \dots, \mathbf{z}_N^{(0)}] \in \mathbb{R}^{(N+1) \times D}.$$

This sequence is processed by L Transformer encoder layers, each consisting of multi-head self-attention (MSA) and feedforward networks (FFN) with layer normalization and residual connections.

Attention Aggregation of the Quality Token: At layer ℓ , each token $\mathbf{z}_i^{(\ell)}$ is projected into queries, keys, and values:

$$\mathbf{q}_i^{(\ell)} = \mathbf{z}_i^{(\ell)} W_Q, \quad \mathbf{k}_i^{(\ell)} = \mathbf{z}_i^{(\ell)} W_K, \quad \mathbf{v}_i^{(\ell)} = \mathbf{z}_i^{(\ell)} W_V,$$

with $W_Q, W_K, W_V \in \mathbb{R}^{D \times d_h}$ and $d_h = D/h$ for h heads. The quality token at position 0 forms attention weights over all tokens:

$$\alpha_{0,j}^{(\ell)} = \frac{\exp\left(\frac{\mathbf{q}_0^{(\ell)} \cdot \mathbf{k}_j^{(\ell)}}{\sqrt{d_h}}\right)}{\sum_{m=0}^N \exp\left(\frac{\mathbf{q}_0^{(\ell)} \cdot \mathbf{k}_m^{(\ell)}}{\sqrt{d_h}}\right)}.$$

The quality token is updated by forming a linear combination of all value vectors, with coefficients determined by the attention distribution:

$$\tilde{\mathbf{z}}_0^{(\ell)} = \sum_{j=0}^N \alpha_{0,j}^{(\ell)} \mathbf{v}_j^{(\ell)}.$$

This is extended to h parallel heads, whose outputs are then concatenated and linearly projected:

$$\mathbf{z}_0^{(\ell+1)} = [\tilde{\mathbf{z}}_0^{(\ell,1)} \| \dots \| \tilde{\mathbf{z}}_0^{(\ell,h)}] W_O, \quad W_O \in \mathbb{R}^{(h \cdot d_h) \times D}.$$

ViT-FIQA: Unlike ViT [11], designed for image classification tasks with a classification token (CLS), the SOTA ViT architecture for FR [9, 38, 48], projects the final token embeddings into D -dimensional embedding space and pass it through margin-penalty softmax loss, which we extended with quality regression. We propose to split the final token sequence into two branches:

- The **quality token** $\mathbf{z}_0^{(L)}$ is used as input for the regression head to predict the scalar quality score $\hat{q} \in \mathbb{R}$, which is optimized through CR-FIQA loss [7].
- The **patch tokens** $\{\mathbf{z}_i^{(L)}\}_{i=1}^N$ are projected into a D -dimensional embedding using a fully-connected layer and used for the FR task, trained with CosFace [46].

The final loss to jointly learn FR and quality prediction is given by:

$$\mathcal{L} = \mathcal{L}_{FR} + \lambda \mathcal{L}_{FIQ},$$

Where \mathcal{L}_{FR} is the FR loss (CosFace [46] loss), \mathcal{L}_{FIQ} is the FIQA regression loss (Smooth L1 between predicted quality and CR-FIQA [7] score), and λ is a weighting factor (set to 10, following [7]) to balance the two objectives. By integrating the quality token directly into the Transformer pipeline, ViT-FIQA leverages the full capacity of ViTs to model face image utility in a principled, scalable manner.

4. Experimental Setup

Datasets: We utilized MS1MV2 [10] to train our ViT-FIQA. MS1MV2 [10] is a refined version of MS-Celeb-

1M [17] dataset. It contains approximately 5.8M images from 85K identities. All images are aligned and cropped to 112×112 using landmarks obtained by the Multi-task Cascaded Convolutional Networks (MTCNN) [50], following [10]. All the training and testing images are normalized to have values between -1 and 1.

Model Training: We utilized ViT-Small [11] backbone. We trained our ViT-FIQA for 34 epochs using AdamW [25, 30] optimizer, with mini-batch size of 1024, base learning rate $1e-3$ ($\beta_1 = 0.9$, $\beta_2 = 0.999$), weight decay 0.05, and polynomial decay scheduling. We applied an extensive data augmentation pipeline, following [25], composed by Affine Transformation (scale, rotation, translation), Cutout / Coarse Dropout, Zero-Padded Random Resized Crop, Brightness Adjustment, Saturation Adjustment, Contrast Adjustment, Sharpness Adjustment, Histogram Equalization, Grayscale Conversion, Average Blur, Gaussian Blur, Motion Blur, Low-Resolution Simulation via Resize, Spatial Warping. We compared the effectiveness of the learnable quality token with respect to the original method proposed by [7], we trained our models with both methods. The former, which employs the novel quality token, will be noted as ViT-FIQA (T). In the latter, noted as ViT-FIQA (C), no additional token has been employed, leaving the final face embedding as input for both the margin-penalty softmax loss and the FIQ regression layer.

Evaluation: We reported the achieved results on seven different benchmarks: Labeled Faces in the Wild (LFW) [20], AgeDB-30 [34], Celebrities in Frontal-Profile in the Wild (CFP-FP) [41], Cross-Age LFW (CALFW) [52], Adience [12], Cross-Pose LFW (CPLFW) [51], and Cross-Quality LFW (XQLFW) [27]. These benchmarks enable a comparative analysis with state-of-the-art (SOTA) FIQA techniques [1, 3, 7, 31] and allow us to assess the robustness of the proposed approach. Performance is assessed via Error-versus-Discard Characteristic (EDC) curves [15], which evaluate the effect of excluding low-quality facial images on verification accuracy. The False Non-Match Rate (FNMR) is measured at set False Match Rate (FMR) thresholds [23], notably $1e-3$, as advised for border security by Frontex [13], and $1e-4$. Furthermore, the Area Under the Curve (AUC) as well as the partial Area Under the Curve (pAUC) of the EDC are reported to assess performance across different rejection rates. The pAUC assesses verification effectiveness by focusing on a specific section of the EDC, up to a rejection rate of 30%, according to [2, 3, 37, 40]. To evaluate the influence of FIQA on varied FR models, we conduct experiments with four CNN-based FR systems: ArcFace [10], ElasticFace (ElasticFace-Arc) [6], MagFace [31], and CurricularFace [21] and two ViT-based FR: SwinFace [38] and TransFace [9], following [3].

5. Experimental Results

This section provides empirical proof of the validity of the use of the quality token together with ViTs to estimate the utility of face samples. Table 1 presents the verification performance as AUC at FMR= $1e-3$ and FMR= $1e-4$, reported on seven benchmarks while experimenting with four FR solutions, Table 2 as partial AUC (30%) at FMR= $1e-3$ and FMR= $1e-4$ reported on the same settings. The EDCs are provided in Figure 2. We compared our results with three IQA approaches, BRISQUE, RankIQA, and DeepIQA, as well as with twelve SOTA FIQA approaches, RankIQ, PFE, SER-FIQ, FaceQnet, MagFace, SDD-FIQA, and CR-FIQA (S and L), DiffFIQA, eDiffFIQA, and GraFIQs (S and L).

Comparison on CNN-based FR: Tables 1 and 2 (first four blocks) present a comprehensive comparison of our proposed ViT-FIQA methods against a diverse set of SOTA FIQA and IQA methods, evaluated under four reference FR backbones (ArcFace, CurricularFace, ElasticFace, and MagFace) across seven benchmarks. The AUC and pAUC (30%) values of the Error vs. Reject Curves (ERC) are reported at two FMR thresholds: $1e-3$ and $1e-4$.

Our results highlight several important patterns. First, IQA baselines consistently underperform compared to all FIQA approaches, confirming that general-purpose perceptual quality does not capture the discriminative utility of facial images in recognition pipelines. This trend is uniform across all FR backbones and operating points.

Second, our proposed ViT-FIQA (T) and ViT-FIQA (C) show strong and stable behavior across the board. They achieve multiple top-3 positions in the rankings, particularly on benchmarks such as Adience, CFP-FP, CPLFW, and XQLFW. This demonstrates that the transformer-based design is competitive with the most recent SOTA approaches, and often closes the gap even under stricter operating points (10^{-4}). Importantly, the methods show consistent transferability across different FR backbones, underlining their robustness as FIQ estimators.

Third, a recurring pattern is that our methods tend to perform best on CFP-FP, CPLFW and Adience, where ViT-FIQA (T/C) often rank first or second. In contrast, our methods most often fall short on AgeDB-30 and CALFW, with CR-FIQA(L) and eDiffFIQA (L) regularly achieving the best results. This suggests that while our models effectively capture intra-class variability caused by pose and image quality, competing methods may be better suited to handle the subtler degradations introduced by large age gaps on specific benchmarks.

Finally, although CR-FIQA(L) and eDiffFIQA(L) often yield the lowest mean pAUC values, our methods consistently remain competitive and within a narrow margin. In several cases, ViT-FIQA (T/C) even tie with or surpass these approaches, particularly on challenging subsets and when

| FR | Method | Adience[12] | | AgeDB-30[34] | | CFP-FP[41] | | LFW[20] | | CALFW[52] | | CPLFW[51] | | XQLFW[27] | | Mean AUC | | | |
|----------------|--------|---------------------|-------------------|-------------------|------------------|------------------|-------------------|-------------------|-------------------|-------------------|-------------------|-------------------|-------------------|------------|--------------------|--------------------|-------------------|-------------------|--------|
| | | 1e-3 | 1e-4 | 1e-3 | 1e-4 | 1e-3 | 1e-4 | 1e-3 | 1e-4 | 1e-3 | 1e-4 | 1e-3 | 1e-4 | 1e-3 | 1e-4 | 1e-3 | 1e-4 | | |
| ArcFace | IQA | BRISQUE[32] | 0.0565 | 0.1289 | 0.0400 | 0.0585 | 0.0344 | 0.0433 | 0.0043 | 0.0049 | 0.0755 | 0.0813 | 0.1755 | 0.2166 | 0.6679 | 0.7122 | 0.0644 | 0.0889 | |
| | IQA | RankIQA[29] | 0.0400 | 0.0933 | 0.0372 | 0.0523 | 0.0301 | 0.0384 | 0.0039 | 0.0045 | 0.0846 | 0.0915 | 0.2437 | 0.2969 | 0.6584 | 0.7039 | 0.0733 | 0.0962 | |
| | IQA | DeepIQA[5] | 0.0568 | 0.1372 | 0.0403 | 0.0523 | 0.0238 | 0.0292 | 0.0049 | 0.0056 | 0.0793 | 0.0850 | 0.2309 | 0.2856 | 0.5958 | 0.6458 | 0.0727 | 0.0991 | |
| | FIOQA | RankIQ[8] | 0.0353 | 0.0873 | 0.0322 | 0.0420 | 0.0152 | 0.0260 | 0.0018 (3) | 0.0024 (3) | 0.0608 | 0.0672 | 0.0633 | 0.0848 | 0.2789 | 0.3332 | 0.0348 | 0.0516 | |
| | FIOQA | PFE[42] | 0.0273 | 0.0483 | 0.0218 | 0.0289 | 0.0287 | 0.0347 | 0.0030 | 0.0038 | 0.0682 | 0.0718 | 0.1343 | 0.1605 | 0.3569 | 0.4187 | 0.0472 | 0.0580 | |
| | FIOQA | SER-FIQ[44] | 0.0223 | 0.0434 | 0.0167 | 0.0223 | 0.0065 | 0.0103 | 0.0023 | 0.0028 | 0.0595 | 0.0627 (3) | 0.0389 | 0.0584 | 0.1812* (1) | 0.2295* (2) | 0.0244 | 0.0333 | |
| | FIOQA | FaceNet[18, 19] | 0.0346 | 0.0734 | 0.0197 | 0.0245 | 0.0240 | 0.0273 | 0.0022 | 0.0027 | 0.0774 | 0.0822 | 0.1504 | 0.1751 | 0.5829 | 0.6136 | 0.0514 | 0.0642 | |
| | FIOQA | MagFace[31] | 0.0207 | 0.0425 | 0.0156 (3) | 0.0198 | 0.0073 | 0.0105 | 0.0016 (2) | 0.0021 (2) | 0.0568 (2) | 0.0602 (2) | 0.0492 | 0.0642 | 0.4022 | 0.4636 | 0.0252 | 0.0332 | |
| | FIOQA | CR-FIQA(S)[7] | 0.0241 | 0.0517 | 0.0144 (1) | 0.0187 (2) | 0.0090 | 0.0145 | 0.0020 | 0.0025 | 0.0521 (1) | 0.0554 (1) | 0.0391 | 0.0567 | 0.2377 | 0.2740 | 0.0234 (2) | 0.0333 | |
| | FIOQA | CR-FIQA(L)[7] | 0.0204 (3) | 0.0353 (1) | 0.0159 | 0.0189 (3) | 0.0050 (2) | 0.0082 (2) | 0.0023 | 0.0029 | 0.0616 | 0.0632 | 0.0360 (2) | 0.0515 (2) | 0.2084 | 0.2441 | 0.0235 | 0.0300 (1) | |
| CurricularFace | IQA | DifFIQ(A)[2] | 0.0251 | 0.0619 | 0.0194 | 0.0262 | 0.0053 (3) | 0.0091 | 0.0020 | 0.0025 | 0.0629 | 0.0688 | 0.0365 | 0.0531 | 0.1847 (2) | 0.2397 (3) | 0.0252 | 0.0369 | |
| | IQA | GraFIQs (S)[28] | 0.0279 | 0.0517 | 0.0247 | 0.0399 | 0.0305 | 0.0398 | 0.0034 | 0.0041 | 0.0787 | 0.0842 | 0.1228 | 0.1573 | 0.5909 | 0.6463 | 0.0480 | 0.0628 | |
| | IQA | GraFIQs (L)[28] | 0.0269 | 0.0429 | 0.0211 | 0.0306 | 0.0292 | 0.0389 | 0.0041 | 0.0047 | 0.0714 | 0.0759 | 0.1120 | 0.1417 | 0.3731 | 0.4234 | 0.0441 | 0.0558 | |
| | IQA | ViT-FIQA (T) (Ours) | 0.0197 (2) | 0.0395 (3) | 0.0177 | 0.0207 | 0.0057 | 0.0084 | 0.0023 | 0.0027 | 0.0593 | 0.0627 | 0.0366 | 0.0519 (3) | 0.1864 (3) | 0.2274 (1) | 0.0235 (3) | 0.0310 (3) | |
| | IQA | ViT-FIQA (C) (Ours) | 0.0195 (1) | 0.0377 (2) | 0.0174 | 0.0225 | 0.0054 | 0.0081 (1) | 0.0023 | 0.0028 | 0.0634 | 0.0666 | 0.0364 (3) | 0.0501 | 0.1914 | 0.2637 | 0.0241 | 0.0316 | |
| | FIOQA | RankIQ[8] | 0.0502 | 0.1097 | 0.0433 | 0.0491 | 0.0326 | 0.0358 | 0.0041 | 0.0047 | 0.0755 | 0.0784 | 0.1441 | 0.1441 | 0.6146 | 0.6336 | 0.0583 | 0.1046 | |
| | FIOQA | RankIQA[29] | 0.0359 | 0.0752 | 0.0394 | 0.0510 | 0.0298 | 0.0356 | 0.0039 | 0.0045 | 0.0808 | 0.0865 | 0.2346 | 0.4654 | 0.5900 | 0.6212 | 0.0707 | 0.1197 | |
| | FIOQA | DeepIQA[5] | 0.0492 | 0.1070 | 0.0407 | 0.0476 | 0.0227 | 0.0278 | 0.0050 | 0.0056 | 0.0764 | 0.0786 | 0.2488 | 0.4961 | 0.5165 | 0.5526 | 0.0738 | 0.1271 | |
| | FIOQA | RankIQ[8] | 0.0314 | 0.0715 | 0.0365 | 0.0417 | 0.0186 | 0.0249 | 0.0018 (3) | 0.0024 (3) | 0.0590 | 0.0640 | 0.0541 | 0.0730 | 0.2449 | 0.2880 | 0.0336 | 0.0462 | |
| | FIOQA | PFE[42] | 0.0265 | 0.0430 | 0.0248 | 0.0275 | 0.0314 | 0.0408 | 0.0032 | 0.0038 | 0.0678 | 0.0705 | 0.1160 | 0.1305 | 0.2948 | 0.3171 | 0.0450 | 0.0527 | |
| ElasticFace | IQA | SER-FIQ[44] | 0.0211 | 0.0381 | 0.0167 | 0.193 (1) | 0.0074 | 0.111 | 0.0025 | 0.0030 | 0.0587 | 0.0610 | 0.0356 | 0.0520 | 0.1558* (1) | 0.1866* (1) | 0.0237 | 0.0307 | |
| | IQA | FaceNet[18, 19] | 0.0326 | 0.0667 | 0.0221 | 0.0267 | 0.0226 | 0.0274 | 0.0022 | 0.0027 | 0.0767 | 0.0799 | 0.1384 | 0.1329 | 0.5035 | 0.5411 | 0.0491 | 0.0870 | |
| | IQA | MagFace[31] | 0.0200 | 0.0364 | 0.0167 (3) | 0.0195 (3) | 0.0078 | 0.1111 | 0.0016 (2) | 0.0021 (2) | 0.0563 (2) | 0.0590 (2) | 0.0449 | 0.0607 | 0.3758 | 0.4178 | 0.0246 | 0.0315 | |
| | IQA | SDD-FIQA[36] | 0.0230 | 0.0462 | 0.0219 | 0.0254 | 0.0138 | 0.0185 | 0.0021 | 0.0027 | 0.0637 | 0.0675 | 0.0465 | 0.0671 | 0.2649 | 0.3053 | 0.0285 | 0.0379 | |
| | IQA | CR-FIQA(S)[7] | 0.0227 | 0.0446 | 0.156 (1) | 0.0198 | 0.0097 | 0.0148 | 0.0020 | 0.0025 | 0.0513 (1) | 0.0534 (1) | 0.0340 | 0.0501 | 0.2101 | 0.2470 | 0.0225 (2) | 0.0309 | |
| | IQA | CR-FIQA(L)[7] | 0.0198 (3) | 0.0336 (2) | 0.0162 (2) | 0.0200 | 0.0054 (2) | 0.0080 (1) | 0.0023 | 0.0029 | 0.0608 | 0.0657 | 0.0305 (2) | 0.0461 (1) | 0.1716 | 0.2318 | 0.0228 (3) | 0.0287 (2) | |
| | IQA | DifFIQ(A)[2] | 0.0230 | 0.0475 | 0.0227 | 0.0260 | 0.0055 (3) | 0.0092 | 0.0020 | 0.0025 | 0.0608 | 0.0657 | 0.0305 (2) | 0.0441 (1) | 0.1600 (2) | 0.1871 (2) | 0.0241 | 0.0325 | |
| | IQA | dDiffIQA(L)[3] | 0.0199 | 0.0383 (3) | 0.0170 | 0.0195 (2) | 0.0048 (1) | 0.0014 (1) | 0.0019 (1) | 0.0056 (3) | 0.0601 (3) | 0.0303 (1) | 0.0455 (2) | 0.1717 | 0.2080 | 0.0217 (1) | 0.0382 (1) | 0.0236 | 0.0296 |
| | FIOQA | RankIQ[8] | 0.0400 | 0.0777 | 0.0309 | 0.0337 | 0.0149 | 0.0180 | 0.0013 (1) | 0.0020 (2) | 0.0598 | 0.0614 | 0.0581 | 0.0727 | 0.2468 | 0.2776 | 0.0342 | 0.0443 | |
| | FIOQA | PFE[42] | 0.0285 | 0.0461 | 0.0216 | 0.0228 | 0.0258 | 0.0314 | 0.0026 | 0.0038 | 0.0670 | 0.0688 | 0.1225 | 0.1408 | 0.3346 | 0.3544 | 0.0447 | 0.0523 | |
| MagFace | IQA | SER-FIQ[44] | 0.0240 | 0.0417 | 0.0163 | 0.0179 | 0.0061 | 0.0085 | 0.0021 | 0.0028 | 0.0574 | 0.0590 | 0.0387 | 0.0513 | 0.1576* (1) | 0.1868* (1) | 0.0241 | 0.0302 | |
| | IQA | FaceNet[18, 19] | 0.0369 | 0.0667 | 0.0194 | 0.0207 | 0.0227 | 0.0247 | 0.0021 | 0.0026 | 0.0763 | 0.0777 | 0.1420 | 0.1480 | 0.2880 | 0.3171 | 0.0450 | 0.0527 | |
| | IQA | MagFace[31] | 0.0225 | 0.0385 | 0.0150 | 0.0158 (2) | 0.0069 | 0.0095 | 0.0014 (3) | 0.0021 (3) | 0.0553 (2) | 0.0563 (2) | 0.0474 | 0.0507 | 0.3973 | 0.4282 | 0.0248 | 0.0303 | |
| | IQA | SDD-FIQA[36] | 0.0277 | 0.0512 | 0.0187 | 0.0200 | 0.0098 | 0.0118 | 0.0019 | 0.0027 | 0.0624 | 0.0638 | 0.0493 | 0.0634 | 0.3052 | 0.3562 | 0.0283 | 0.0355 | |
| | IQA | CR-FIQA(S)[7] | 0.0257 | 0.0446 | 0.0146 (2) | 0.0160 | 0.0070 | 0.0096 | 0.0015 | 0.0022 | 0.0509 (1) | 0.0522 (1) | 0.0383 | 0.0502 | 0.2835 | 0.3203 (3) | 0.0230 | 0.0294 | |
| | IQA | CR-FIQA(L)[7] | 0.0214 (2) | 0.0352 (2) | 0.0149 (3) | 0.0195 (3) | 0.0045 (2) | 0.0065 (1) | 0.0018 | 0.0025 | 0.0594 | 0.0608 | 0.0350 (3) | 0.0462 | 0.1798 | 0.2060 | 0.0228 (2) | 0.0279 (2) | |
| | IQA | DifFIQ(A)[2] | 0.0278 | 0.0536 | 0.0194 | 0.0207 | 0.0050 | 0.0073 | 0.0019 | 0.0025 | 0.0616 | 0.0634 | 0.0350 (2) | 0.0445 (2) | 0.1599 (2) | 0.1890 (2) | 0.0248 | 0.0320 | |
| | IQA | dDiffIQA(L)[3] | 0.0222 | 0.0374 | 0.193 (1) | 0.148 (1) | 0.0043 (1) | 0.0012 (2) | 0.0019 (1) | 0.0564 (3) | 0.0576 (3) | 0.0323 (1) | 0.0440 (1) | 0.1688 | 0.1996 (3) | 0.0217 (1) | 0.0370 (1) | 0.0236 | 0.0320 |
| | IQA | GraFIQs (S)[28] | 0.0297 | 0.0512 | 0.0265 | 0.0303 | 0.0236 | 0.0322 | 0.0031 | 0.0041 | 0.0773 | 0.0791 | 0.1209 | 0.1395 | 0.3854 | 0.4414 | 0.0468 | 0.0561 | |
| | IQA | GraFIQs (L)[28] | 0.0280 | 0.0430 | 0.0201 | 0.0224 | 0.0245 | 0.0292 | 0.0037 | 0.0046 | 0.0695 | 0.0711 | 0.1035 | 0.1231 | 0.3598 | 0.3963 | 0.0416 | 0.0489 | |
| SwiftFace | IQA | ViT-FIQA (T) (Ours) | 0.0214 (3) | 0.0362 (3) | 0.0169 | 0.0209 | 0.0179 | 0.0052 | 0.0017 | 0.0023 | 0.0575 | 0.0608 | 0.0352 | 0.0462 | 0.1679 | 0.2174 | 0.0230 | 0.0282 (3) | |
| | IQA | ViT-FIQA (C) (Ours) | 0.0211 (1) | 0.0351 (1) | 0.0167 | 0.0201 | 0.0062 | 0.0080 (1) | 0.0023 | 0.0028 | 0.0614 | 0.0628 | 0.0374 (3) | 0.0468 | 0.2369 | 0.2839 | 0.0243 | 0.0337 (1) | |
| | FIOQA | RankIQ[8] | 0.0594 | 0.1309 | 0.0442 | 0.0799 | 0.0422 | 0.0589 | 0.0043 | 0.0058 | 0.0758 | 0.0788 | 0.2916 | 0.3097 | 0.6911 | 0.7229 | 0.0863 | 0.1440 | |
| | FIOQA | RankIQA[29] | 0.0407 | 0.0889 | 0.0370 | 0.0681 | 0.0543 | 0.0404 | 0.0056 | 0.0056 | 0.0829 | 0.0857 | 0.3251 | 0.6475 | 0.6706 | 0.7046 | 0.0878 | 0.1583 | |
| | FIOQA | DeepIQA[5] | 0.0571 | 0.1302 | 0.0417 | 0.0721 | 0.0322 | 0.0545 | 0.0048 | 0.0059 | 0.0787 | 0.0809 | 0.3672 | 0.6632 | 0.6162 | 0.6519 | 0.0969 | 0.1678 | |
| | FIOQA | RankIQ[8] | 0.0359 | 0.0837 | 0.0361 | 0.0531 | 0.0213 | 0.0332 | 0.0019 (3) | 0.0027 | 0.0602 | 0.0629 | 0.0659 | 0.1642 | 0.3076 | 0.3475 | 0.0369 | 0.0666 | |
| | FIOQA | PFE[42] | 0.0283 | 0.0481 | 0.0244 | 0.0401 | 0.0398 | 0.0625 | 0.0029 | 0.0035 | 0.0680 | 0.0691 | 0.1357 | 0.1815 | 0.4089 | 0.4472 | 0.0499 | 0.0675 | |
| | FIOQA | SER-FIQ[44] | 0.0233 | 0.0451 | 0.0185 | 0.0293 | 0.0080 | 0.0139 | 0.0025 | 0.0033 | 0.0590 | 0.0607 | 0.0397 | 0.0821 | 0.2139* (1) | 0.2562* (1) | 0.0252 | 0.0391 | |
| | FIOQA | FaceNet[18, 19] | 0.0365 | | | | | | | | | | | | | | | | |

| FR | Method | Adience[12] | | AgeDB-30[34] | | CFP-FP[41] | | LFW[20] | | CALFW[52] | | CPLFW[51] | | XQLFW[27] | | Mean pAUC | |
|----------------|---------------------|-------------------|-------------------|-------------------|-------------------|-------------------|-------------------|-------------------|-------------------|-------------------|-------------------|-------------------|-------------------|-------------------|-------------------|-------------------|-------------------|
| | | 1e-3 | 1e-4 |
| ArcFace | BRISQUE[32] | 0.0143 | 0.0333 | 0.0096 | 0.0146 | 0.0096 | 0.0136 | 0.0099 | 0.0010 | 0.0200 | 0.0225 | 0.0480 | 0.0624 | 0.1512 | 0.1689 | 0.0171 | 0.0246 |
| | RankIQA[29] | 0.0124 | 0.0302 | 0.0087 | 0.0141 | 0.0088 | 0.0135 | 0.0099 | 0.0010 | 0.0209 | 0.0234 | 0.0506 | 0.0658 | 0.1532 | 0.1709 | 0.0170 | 0.0247 |
| | DeepIQA[5] | 0.0145 | 0.0337 | 0.0093 | 0.0140 | 0.0088 | 0.0119 | 0.0099 | 0.0010 | 0.0207 | 0.0230 | 0.0504 | 0.0653 | 0.1487 | 0.1668 | 0.0175 | 0.0248 |
| | RankIQ[8] | 0.0125 | 0.0304 | 0.0090 | 0.0143 | 0.0071 | 0.0114 | 0.0066 | 0.0008 | 0.0191 | 0.0215 | 0.0306 | 0.0427 | 0.1270 | 0.1500 | 0.0132 | 0.0202 |
| | PFE[42] | 0.0100 | 0.0229 | 0.0080 | 0.0123 | 0.0089 | 0.0124 | 0.0099 | 0.0010 | 0.0192 | 0.0211 | 0.0351 | 0.0470 | 0.1064 (1) | 0.1284 (2) | 0.0137 | 0.0195 |
| | SER-FIQ[44] | 0.0102 | 0.0244 | 0.0066 | 0.0107 | 0.0035 | 0.0057 | 0.0007 | 0.0008 | 0.0187 | 0.0205 | 0.0199 | 0.0319 | 0.1175* (3) | 0.1385* (3) | 0.0099 | 0.0157 |
| CurricularFace | FaceNet[18, 19] | 0.0130 | 0.0303 | 0.0076 | 0.0113 | 0.0077 | 0.0100 | 0.0008 | 0.0009 | 0.0196 | 0.0216 | 0.0428 | 0.0554 | 0.1523 | 0.1686 | 0.0153 | 0.0216 |
| | MagFace[31] | 0.0099 | 0.0247 | 0.0065 (2) | 0.0098 | 0.0045 | 0.0068 | 0.0006 (1) | 0.0007 (3) | 0.0177 (2) | 0.0193 (2) | 0.0249 | 0.0360 | 0.1359 | 0.1614 | 0.0107 | 0.0162 |
| | FIOQA | 0.0104 | 0.0259 | 0.0073 | 0.0088 (2) | 0.0068 | 0.0109 | 0.0007 | 0.0009 | 0.0188 | 0.0205 | 0.0279 | 0.0377 | 0.1356 | 0.1525 | 0.0120 | 0.0174 |
| | CR-FIQA(S)[7] | 0.0101 | 0.0257 | 0.0068 | 0.0100 | 0.0042 | 0.0078 | 0.0006 | 0.0008 | 0.0178 | 0.0197 (3) | 0.0207 | 0.0324 | 0.1242 | 0.1391 | 0.0100 | 0.0161 |
| | DifFIQ(A R)[2] | 0.0097 | 0.0201 (2) | 0.0066 (3) | 0.0089 (3) | 0.0035 (3) | 0.0058 | 0.0007 | 0.0009 | 0.0177 (1) | 0.0186 (1) | 0.0190 (3) | 0.0307 (1) | 0.1213 | 0.1378 | 0.0095 (2) | 0.0142 (1) |
| | dDifFIQ(A)L[3] | 0.0090 (3) | 0.0230 | 0.0060 (1) | 0.0079 (1) | 0.0033 (1) | 0.0056 (3) | 0.0007 (1) | 0.0177 (3) | 0.0199 | 0.0189 (2) | 0.0058 (2) | 0.1223 | 0.1474 | 0.0093 (1) | 0.0147 (2) | |
| ElasticFace | GraFIQs (S) [28] | 0.0118 | 0.0262 | 0.0082 | 0.0142 | 0.0095 | 0.0138 | 0.0008 | 0.0009 | 0.0209 | 0.0235 | 0.0361 | 0.0496 | 0.1204 | 0.1354 (3) | 0.0146 | 0.0213 |
| | GraFIQs (L) [28] | 0.0097 | 0.0198 (1) | 0.0069 | 0.0113 | 0.0091 | 0.0135 | 0.0010 | 0.0011 | 0.0194 | 0.0218 | 0.0344 | 0.0472 | 0.1065 (2) | 0.1282 (1) | 0.0134 | 0.0191 |
| | ViT-FIQA (T) (Ours) | 0.0089 (1) | 0.0231 | 0.0069 | 0.0093 | 0.0033 (2) | 0.0054 (1) | 0.0006 | 0.0007 | 0.0184 | 0.0200 | 0.0191 | 0.0309 | 0.1224 | 0.1364 | 0.0096 (3) | 0.0149 (3) |
| | ViT-FIQA (C) (Ours) | 0.0090 (2) | 0.0226 (3) | 0.0074 | 0.0112 | 0.0035 | 0.0055 (2) | 0.0007 | 0.0008 | 0.0189 | 0.0205 | 0.0191 | 0.0311 | 0.1218 | 0.1583 | 0.0098 | 0.0153 |
| | RankIQA[29] | 0.0126 | 0.0283 | 0.0100 | 0.0124 | 0.0094 | 0.0107 | 0.0009 | 0.0010 | 0.0196 | 0.0211 | 0.0370 | 0.1161 | 0.1345 | 0.1444 | 0.0149 | 0.0316 |
| | DeepIQA[5] | 0.0109 | 0.0254 | 0.0091 | 0.0122 | 0.0095 | 0.0127 | 0.0009 | 0.0010 | 0.0202 | 0.0219 | 0.0411 | 0.1198 | 0.1361 | 0.1461 | 0.0153 | 0.0322 |
| MagFace | RankIQ[8] | 0.0107 | 0.0247 | 0.0096 | 0.0118 | 0.0078 | 0.0107 | 0.0006 | 0.0008 | 0.0182 | 0.0200 | 0.0275 | 0.0402 | 0.1129 | 0.1292 | 0.0124 | 0.0181 |
| | PFE[42] | 0.0099 | 0.0192 | 0.0089 | 0.0107 | 0.0090 | 0.0121 | 0.0009 | 0.0010 | 0.0185 | 0.0198 | 0.0316 | 0.0444 | 0.0941 (1) | 0.1054 (1) | 0.0130 | 0.0179 |
| | SER-FIQ[44] | 0.0091 | 0.0207 | 0.0067 (3) | 0.0083 | 0.0035 (3) | 0.0053 (1) | 0.0007 | 0.0008 | 0.0179 | 0.0192 | 0.0169 | 0.0308 | 0.1054* (3) | 0.1217* (3) | 0.0091 | 0.0142 |
| | FaceNet[18, 19] | 0.0116 | 0.0254 | 0.0082 | 0.0101 | 0.0074 | 0.0099 | 0.0008 | 0.0009 | 0.0191 | 0.0204 | 0.0355 | 0.1066 | 0.1322 | 0.1459 | 0.0138 | 0.0289 |
| | MagFace[31] | 0.0089 | 0.0198 | 0.0066 (1) | 0.0082 (2) | 0.0048 | 0.0068 | 0.0006 (1) | 0.0007 (3) | 0.0175 | 0.0185 (2) | 0.0219 | 0.0357 | 0.1257 | 0.1373 | 0.0101 | 0.0149 |
| | FIOQA | 0.0115 | 0.0224 | 0.0080 | 0.0098 | 0.0073 | 0.0097 | 0.0007 | 0.0008 | 0.0183 | 0.0197 | 0.0237 | 0.0413 | 0.1219 | 0.1372 | 0.0112 | 0.0171 |
| SwiftFace | CR-FIQA(S)[7] | 0.0088 | 0.0211 | 0.0071 | 0.0089 | 0.0047 | 0.0067 | 0.0006 | 0.0008 | 0.0174 | 0.0186 | 0.0274 | 0.0437 | 0.1138 | 0.1304 | 0.0109 | 0.0147 |
| | CR-FIQA(L)[7] | 0.0089 | 0.0221 | 0.0072 | 0.0083 | 0.0050 | 0.0067 | 0.0006 | 0.0008 | 0.0173 | 0.0186 | 0.0273 | 0.0437 | 0.1140 | 0.1313 | 0.0113 | 0.0153 |
| | DifFIQ(A R)[2] | 0.0087 | 0.0206 | 0.0087 | 0.0104 | 0.0054 | 0.0054 (3) | 0.0006 | 0.0007 | 0.0178 | 0.0196 | 0.0270 | 0.0437 | 0.1109 | 0.1250 | 0.0092 | 0.0141 |
| | dDifFIQ(A)L[3] | 0.0079 (1) | 0.0182 (2) | 0.0067 | 0.0081 (1) | 0.0034 (1) | 0.0053 (2) | 0.0006 (3) | 0.0007 (1) | 0.0172 (1) | 0.0186 | 0.0316 | 0.0498 | 0.1129 | 0.1267 | 0.0086 (1) | 0.0135 (2) |
| | GraFIQs (S) [28] | 0.0109 | 0.0227 | 0.0089 | 0.0122 | 0.0093 | 0.0122 | 0.0008 | 0.0009 | 0.0203 | 0.0219 | 0.0326 | 0.0459 | 0.1098 | 0.1238 | 0.0193 | 0.0245 |
| | GraFIQs (L) [28] | 0.0091 | 0.0181 (1) | 0.0071 | 0.0096 | 0.0092 | 0.0122 | 0.0010 | 0.0011 | 0.0189 | 0.0204 | 0.0309 | 0.0437 | 0.1098 | 0.1238 | 0.0138 | 0.0193 |
| TransFace | ViT-FIQA (T) (Ours) | 0.0102 (1) | 0.0188 (3) | 0.0071 | 0.0098 | 0.0034 (3) | 0.0063 (3) | 0.0005 (3) | 0.0007 | 0.0175 (3) | 0.0186 | 0.0275 (3) | 0.0437 | 0.1094 | 0.1250 | 0.0092 | 0.0141 |
| | ViT-FIQA (C) (Ours) | 0.0103 (1) | 0.0221 (3) | 0.0071 | 0.0163 | 0.0045 (2) | 0.0050 (2) | 0.0009 | 0.0007 | 0.0188 | 0.0194 | 0.0211 | 0.0404 | 0.1084 | 0.1248 | 0.0091 | 0.0131 |
| | RankIQA[29] | 0.0147 | 0.0334 | 0.0101 | 0.0207 | 0.0117 | 0.0205 | 0.0099 | 0.0013 | 0.0199 | 0.0211 | 0.0376 | 0.1163 | 0.1342 | 0.1411 | 0.0167 | 0.0294 |
| | DeepIQA[5] | 0.0128 | 0.0291 | 0.0092 | 0.0212 | 0.0119 | 0.0207 | 0.0099 | 0.0013 | 0.0203 | 0.0209 | 0.0433 | 0.1086 | 0.1428 | 0.1661 | 0.0158 | 0.0297 |
| | RankIQ[8] | 0.0162 | 0.0308 | 0.0098 | 0.0204 | 0.0100 | 0.0208 | 0.0097 | 0.0010 | 0.0201 | 0.0208 | 0.0431 | 0.1082 | 0.1379 | 0.1621 | 0.0161 | 0.0301 |
| | FIOQA | 0.0139 | 0.0276 | 0.0089 | 0.0097 | 0.0067 | 0.0085 | 0.0005 (2) | 0.0008 | 0.0182 | 0.0188 | 0.0291 | 0.0394 | 0.1163 | 0.1342 | 0.1411 | 0.0157 |
| SwiftFace | PFE[42] | 0.0109 | 0.0200 | 0.0077 | 0.0083 | 0.0078 | 0.0103 | 0.0008 | 0.0010 | 0.0184 | 0.0192 | 0.0340 | 0.0438 | 0.1012 (2) | 0.1107 (1) | 0.0133 | 0.0172 |
| | SER-FIQ[44] | 0.0114 | 0.0227 | 0.0064 | 0.0072 | 0.0031 | 0.0044 (3) | 0.0006 | 0.0008 | 0.0177 | 0.0184 | 0.0318 | 0.0429 | 0.1057* (3) | 0.1283* (3) | 0.0096 | 0.0138 |
| | FaceNet[18, 19] | 0.0143 | 0.0274 | 0.0075 | 0.0082 | 0.0071 | 0.0084 | 0.0007 | 0.0009 | 0.0189 | 0.0196 | 0.0371 | 0.0451 | 0.1051 | 0.1264 | 0.0143 | 0.0266 |
| | MagFace[31] | 0.0110 | 0.0211 | 0.0060 (2) | 0.0084 (2) | 0.0043 | 0.0059 | 0.0005 (1) | 0.0007 (3) | 0.0173 | 0.0177 | 0.0237 | 0.0345 | 0.1331 | 0.1445 | 0.0105 | 0.0144 |
| | SDD-FIQA[36] | 0.0116 | 0.0257 | 0.0081 | 0.0122 | 0.0083 | 0.0128 | 0.0007 | 0.0008 | 0.0181 | 0.0186 | 0.0255 | 0.0377 | 0.1336 | 0.1564 | 0.0114 | 0.0158 |
| | CR-FIQA(S)[7] | 0.0103 | 0.0246 | 0.0074 | 0.0137 | 0.0054 | 0.0068 (2) | 0.0007 | 0.0010 | 0.0177 (2) | 0.0182 (2) | 0.0225 | 0.0348 | 0.1356 | 0.1539 | 0.0106 | 0.0198 |
| TransFace | CR-FIQA(L)[7] | 0.0100 | 0.0210 (2) | 0.0071 (3) | 0.0128 (3) | 0.0048 | 0.0061 (1) | 0.0007 | 0.0008 | 0.0173 (3) | 0.0183 (3) | 0.0209 (3) | 0.0454 (1) | 0.1296 | 0.1506 | 0.0102 (3) | 0.0174 (1) |
| | DifFIQ(A R)[2] | 0.0103 | 0.0251 | 0.0086 | 0.0171 | 0.0047 | 0.0104 | 0.0006 (1) | 0.0008 | 0.0185 | 0.0194 | 0.0207 (1) | 0.0598 | 0.1280 | 0.1501 | 0.0106 | 0.0221 |
| | dDifFIQ(A)L[3] | 0.0093 (3) | 0.0224 | 0.0067 (2) | 0.0113 (1) | 0.0042 (1) | 0.0007 | 0.0006 (3) | 0.0082 (2) | 0.0177 (1) | 0.0182 (1) | 0.0212 | 0.0359 | 0.1323 | 0.1498 | 0.0100 (1) | 0.0203 |
| | GraFIQs (S) [28] | 0.0126 | 0.0268 | 0.0095 | 0.0115 | 0.0020 | 0.0088 | 0.0008 | 0.0011 | 0.0209 | 0.0219 | 0.0387 | 0.0637 | 0.1298 | 0.1556 | 0.0156 | 0.0258 |
| | GraFIQs (L) [28] | 0.0103 | 0.0203 (1) | 0.0074 | 0.0174 | 0.0116 | 0.0181 | 0.0010 | 0.0014 | 0.0195 | 0.0202 | 0.0368 | 0.0617 | 0.1189 (1) | 0.1374 (2) | 0.0144 | 0.0232 |
| | ViT-FIQA (T) (Ours) | 0.0091 (2) | 0.0229 | 0.0073 | 0.0134 | 0.0046 | 0.0071 (3) | 0.0006 | 0.0008 (3) | 0.0182 | 0.0188 | 0.0208 (2) | 0.0454 (2) | 0.1316 | 0.1500 | 0.0101 (2) | 0.0181 (2) |
| SwiftFace | ViT-FIQA (C) (Ours) | 0.0091 (1) | 0.0221 (3) | 0.0077 | 0.0163 | 0.0045 (2) | 0.0055 (2) | 0.0007 | 0.0008 | 0.0188 | 0.0194 | 0.0211 | 0.0459 (3) | 0.1286 | 0.1497 | 0.0103 | 0.0189 (3) |
| | RankIQA[29] | 0.0204 | 0.0431 | 0.0120 | 0.0146 | 0.0025 | 0.0070 | 0.0009 | | | | | | | | | |

evaluated under stricter operating points, highlighting the potential on challenging and maintain strong overall competitiveness across backbones.

Comparison on ViT-based FR: Tables 1 and 2 (last two blocks) present the AUCs and pAUCs (30%) of EDC under ViT-based FR backbones. As in the CNN-based experiments, IQA baselines perform considerably worse than all FIQA approaches, confirming once again that generic image quality measures are misaligned with FR performance.

For SwinFace, our proposed methods perform strongly. ViT-FIQA (C) achieves the best performance on Adience at both operating points (exception made for pAUC under $FMR=1e34$), and provides the lowest values on XQLFW with the same pattern, outperforming all competing methods including SER-FIQ. ViT-FIQA (T) follows closely, ranking second or third on Adience, CFP-FP, and XQLFW. On CFP-FP at 10^{-3} , both variants are competitive but

slightly behind CR-FIQA and eDiffFIQA. Overall, the mean pAUC values of ViT-FIQA (T) are always in the top 3 positions under this backbone .

For TransFace, ViT-FIQA (C) achieves the best performance on Adience at both operating points (exception made for pAUC under $FMR=1e34$) and ranks first on XQLFW, while ViT-FIQA (T) secures second or third place on the same benchmarks. On CFP-FP, both variants remain extremely competitive with CR-FIQA(L) and eDiffFIQA (L). In terms of mean pAUC, our ViT-FIQA (T) consistently achieves the second or third best results, tightly following CR-FIQA (L) and eDiffFIQA (L).

A consistent pattern emerges across both ViT-based backbones: our methods excel on Adience and XQLFW, often taking the top rank, and they maintain strong competitiveness on pose-related benchmarks such as CFP-FP and CPLFW. In contrast, on AgeDB-30 and CALFW, ViT-FIQA (T/C) regularly fall behind CR-FIQA (L) and eDiffFIQA

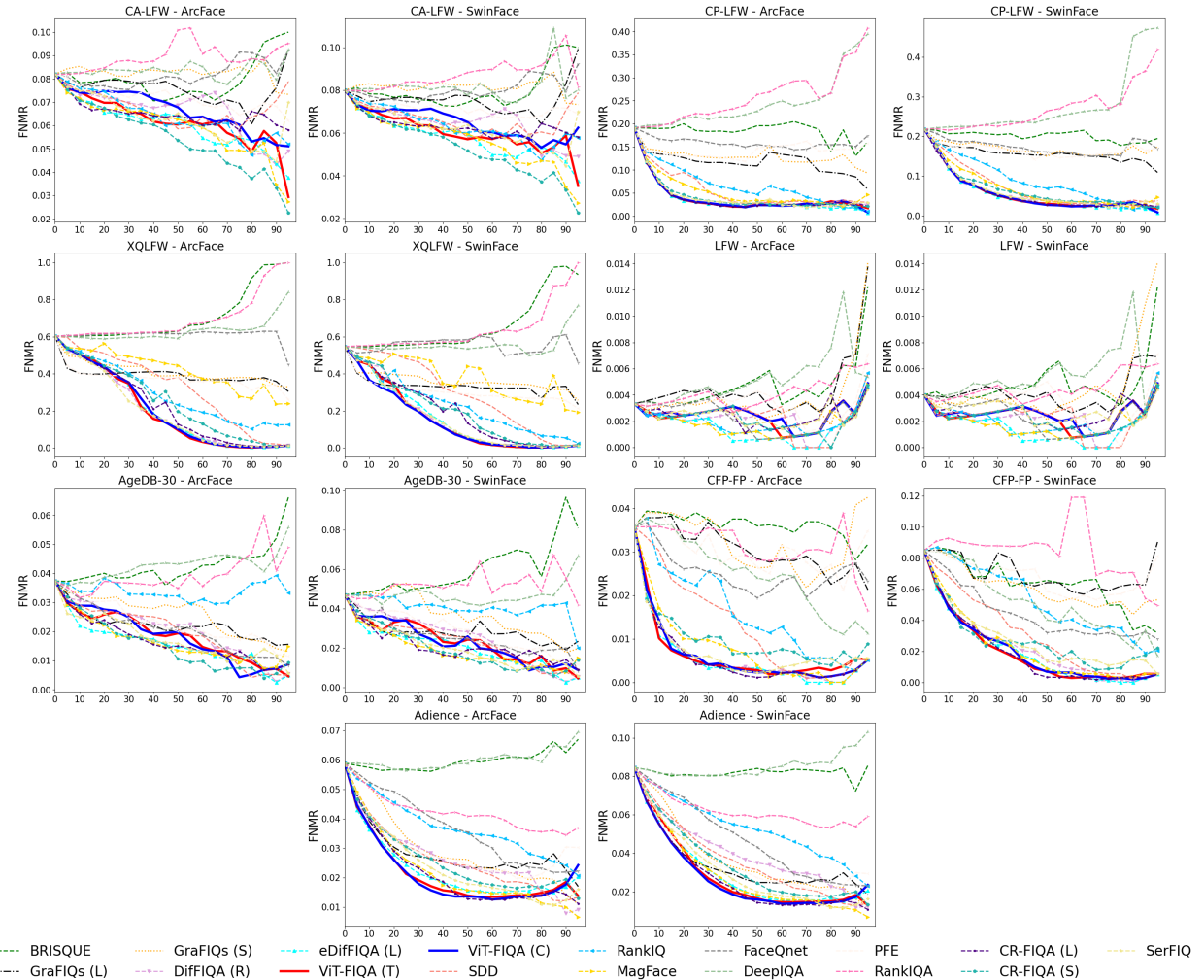


Figure 2. EDC curves for FNMR@ $FMR=1e-3$ for all evaluated benchmarks using CNN-based (ArcFace) and ViT-based (SwinFace) FR models. The proposed ViT-FIQA (T) is shown in solid red, ViT-FIQA (C) is shown in solid blue.

(L), echoing the trend observed in the CNN-based experiments and confirming that our approach generalizes effectively across both CNN- and ViT-based recognition models, while also indicating that age-related variability remains the most challenging condition.

6. Conclusions

In this work, we introduced ViT-FIQQA, a novel Vision Transformer-based approach for FIQQA. By augmenting standard ViT architectures with a dedicated, learnable quality token, our method effectively captures global contextual information across facial regions and predicts a scalar quality score aligned with the FR task. The integration of a classifiability-related loss ensures that the learned quality scores reflect the relative discriminability of facial images, maintaining a tight coupling with the underlying recognition pipeline. Our extensive experiments across multiple benchmarks and diverse FR models, spanning both CNN-

based and transformer-based architectures, demonstrate the robustness and generalizability of ViT-FIQQA. The method consistently ranks among the top performers, particularly excelling in challenging datasets like Adience, CFP-FP, CPLFW and XQLFW. These results highlight the potential of leveraging transformer-based architectures for FIQQA, while highlighting limitations on specific benchmarks like AgeDB-30 and CALFW.

Acknowledgments This research work has been funded by the German Federal Ministry of Education and Research and the Hessen State Ministry for Higher Education, Research and the Arts within their joint support of the National Research Center for Applied Cybersecurity ATHENE. This work was carried out during the tenure of an ERCIM ‘Alain Bensoussan’ Fellowship Programme.

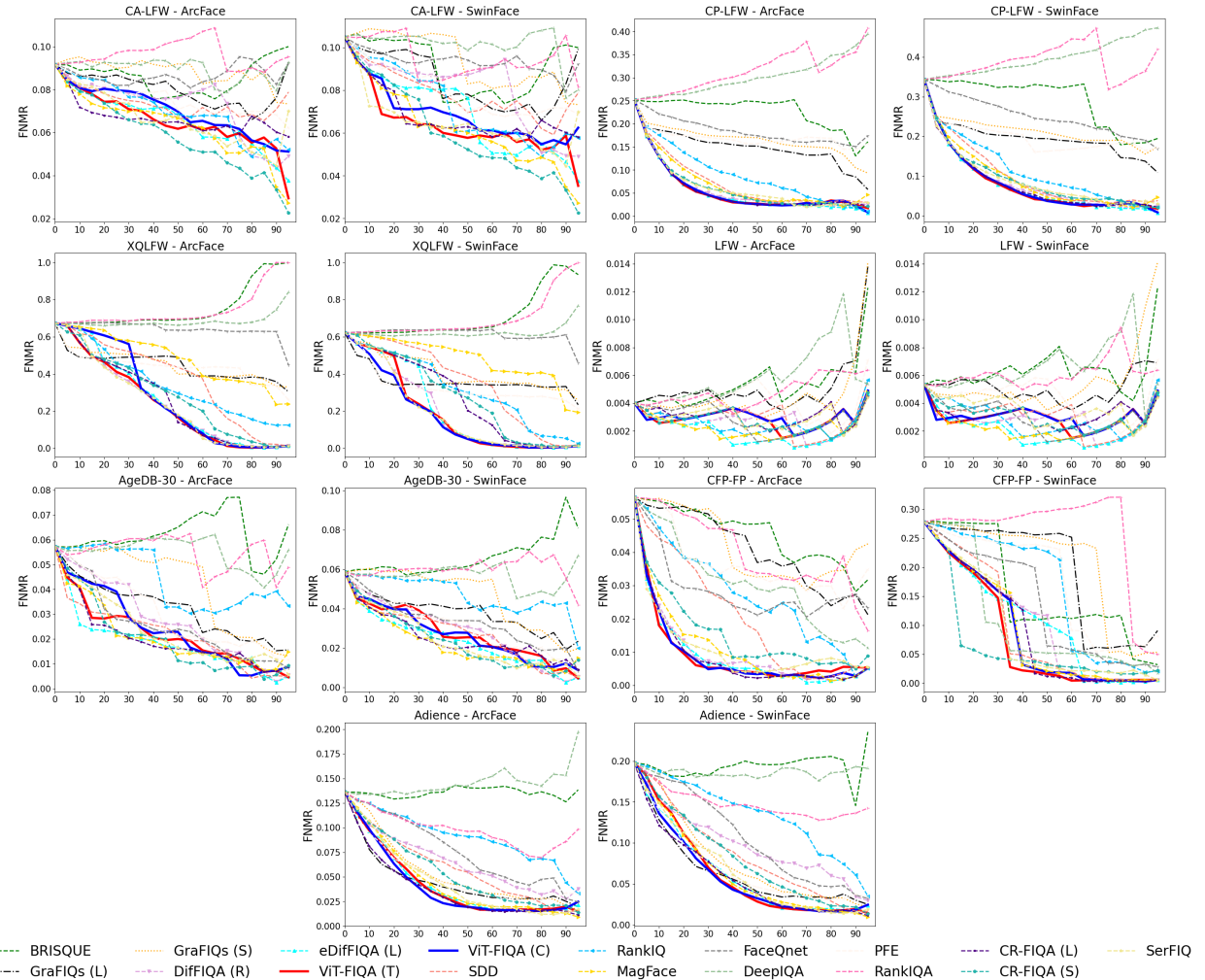


Figure 3. EDC curves for FNMR@FMR=1e-4 for all evaluated benchmarks using CNN-based (ArcFace) and ViT-based (SwinFace) FR models. The proposed ViT-FIQQA (T) is shown in **solid red**, ViT-FIQQA (C) is shown in **solid blue**.

References

- [1] Žiga Babnik, Naser Damer, and Vitomir Štruc. Optimization-based improvement of face image quality assessment techniques. In *11th International Workshop on Biometrics and Forensics, IWBF 2023, Barcelona, Spain, April 19-20, 2023*, pages 1–6. IEEE, 2023. [1](#), [4](#)
- [2] Žiga Babnik, Peter Peer, and Vitomir Štruc. Diffiq: Face image quality assessment using denoising diffusion probabilistic models. In *2023 IEEE International Joint Conference on Biometrics (IJCB)*, pages 1–10, 2023. [2](#), [4](#), [5](#), [6](#)
- [3] Žiga Babnik, Peter Peer, and Vitomir Štruc. eDifFIQA: Towards Efficient Face Image Quality Assessment based on Denoising Diffusion Probabilistic Models. *IEEE Transactions on Biometrics, Behavior, and Identity Science (TBIOM)*, 2024. [2](#), [4](#), [5](#), [6](#)
- [4] Lacey Best-Rowden and Anil K. Jain. Learning face image quality from human assessments. *IEEE Trans. Inf. Forensics Secur.*, 13(12):3064–3077, 2018. [2](#)
- [5] Sebastian Bosse, Dominique Maniry, Klaus-Robert Müller, Thomas Wiegand, and Wojciech Samek. Deep neural networks for no-reference and full-reference image quality assessment. *IEEE Trans. Image Process.*, 27(1):206–219, 2018. [5](#), [6](#)
- [6] Fadi Boutros, Naser Damer, Florian Kirchbuchner, and Arjan Kuijper. Elasticface: Elastic margin loss for deep face recognition. In *IEEE/CVF Conference on Computer Vision and Pattern Recognition Workshops, CVPR Workshops 2022, New Orleans, LA, USA, June 19-20, 2022*, pages 1577–1586. IEEE, 2022. [4](#)
- [7] Fadi Boutros, Meiling Fang, Marcel Klemt, Biying Fu, and Naser Damer. CR-FIQA: face image quality assessment by learning sample relative classifiability. In *IEEE/CVF Conference on Computer Vision and Pattern Recognition, CVPR 2023, Vancouver, BC, Canada, June 17-24, 2023*, pages 5836–5845. IEEE, 2023. [1](#), [2](#), [3](#), [4](#), [5](#), [6](#)
- [8] Jiansheng Chen, Yu Deng, Gaocheng Bai, and Guangda Su. Face image quality assessment based on learning to rank. *IEEE Signal Process. Lett.*, 22(1):90–94, 2015. [2](#), [5](#), [6](#)
- [9] Jun Dan, Yang Liu, Haoyu Xie, Jiankang Deng, Haoran Xie, Xuansong Xie, and Baigui Sun. Transface: Calibrating transformer training for face recognition from a data-centric perspective. In *ICCV*, pages 20585–20596, 2023. [2](#), [3](#), [4](#)
- [10] Jiankang Deng, Jia Guo, Niannan Xue, and Stefanos Zafeiriou. Arcface: Additive angular margin loss for deep face recognition. In *IEEE Conference on Computer Vision and Pattern Recognition, CVPR 2019, Long Beach, CA, USA, June 16-20, 2019*, pages 4690–4699. Computer Vision Foundation / IEEE, 2019. [3](#), [4](#)
- [11] Alexey Dosovitskiy, Lucas Beyer, Alexander Kolesnikov, Dirk Weissenborn, Xiaohua Zhai, Thomas Unterthiner, Mostafa Dehghani, Matthias Minderer, Georg Heigold, Sylvain Gelly, Jakob Uszkoreit, and Neil Houlsby. An image is worth 16x16 words: Transformers for image recognition at scale. In *9th International Conference on Learning Representations, ICLR 2021, Virtual Event, Austria, May 3-7, 2021*. OpenReview.net, 2021. [2](#), [3](#), [4](#)
- [12] Eran Eidinger, Roee Enbar, and Tal Hassner. Age and gender estimation of unfiltered faces. *IEEE Trans. Inf. Forensics Secur.*, 9(12):2170–2179, 2014. [4](#), [5](#), [6](#)
- [13] Frontex. Best practice technical guidelines for automated border control (abc) systems, 2015. [4](#)
- [14] Biying Fu, Cong Chen, Olaf Henniger, and Naser Damer. A deep insight into measuring face image utility with general and face-specific image quality metrics. In *IEEE/CVF Winter Conference on Applications of Computer Vision, WACV 2022, Waikoloa, HI, USA, January 3-8, 2022*, pages 1121–1130. IEEE, 2022. [1](#)
- [15] P. Grother and E. Tabassi. Performance of biometric quality measures. *IEEE Trans. on Pattern Analysis and Machine Intelligence*, 29(4):531–543, 2007. [4](#)
- [16] P. Grother, M. Ngan A. Hom, and K. Hanaoka. Ongoing face recognition vendor test (frvt) part 5: Face image quality assessment (4th draft). In *National Institute of Standards and Technology. Tech. Rep.*, Sep. 2021. [1](#)
- [17] Yandong Guo, Lei Zhang, Yuxiao Hu, Xiaodong He, and Jianfeng Gao. Ms-celeb-1m: A dataset and benchmark for large-scale face recognition. In *Computer Vision - ECCV 2016 - 14th European Conference, Amsterdam, The Netherlands, October 11-14, 2016, Proceedings, Part III*, pages 87–102. Springer, 2016. [4](#)
- [18] Javier Hernandez-Ortega, Javier Galbally, Julian Fierrez, Rudolf Haraksim, and Laurent Beslay. Faceqnet: Quality assessment for face recognition based on deep learning. In *2019 International Conference on Biometrics, ICB 2019, Crete, Greece, June 4-7, 2019*, pages 1–8. IEEE, 2019. [5](#), [6](#)
- [19] Javier Hernandez-Ortega, Javier Galbally, Julian Fierrez, and Laurent Beslay. Biometric quality: Review and application to face recognition with faceqnet. *CoRR*, abs/2006.03298, 2020. [2](#), [5](#), [6](#)
- [20] Gary B. Huang, Manu Ramesh, Tamara Berg, and Erik Learned-Miller. Labeled faces in the wild: A database for studying face recognition in unconstrained environments. Technical Report 07-49, University of Massachusetts, Amherst, 2007. [4](#), [5](#), [6](#)
- [21] Yuge Huang, Yuhan Wang, Ying Tai, Xiaoming Liu, Pengcheng Shen, Shaolin Li, Jilin Li, and Feiyue Huang. Curricularface: Adaptive curriculum learning loss for deep face recognition. In *2020 IEEE/CVF Conference on Computer Vision and Pattern Recognition, CVPR 2020, Seattle, WA, USA, June 13-19, 2020*, pages 5900–5909. Computer Vision Foundation / IEEE, 2020. [4](#)
- [22] ISO/IEC JTC1 SC37 Biometrics. ISO/IEC 29794-1:2016 Information technology - Biometric sample quality - Part 1: Framework. International Organization for Standardization, 2016. [1](#)
- [23] ISO/IEC JTC1 SC37 Biometrics. ISO/IEC 19795-1:2021 Information technology — Biometric performance testing and reporting — Part 1: Principles and framework. International Organization for Standardization, 2021. [4](#)
- [24] Geunsu Kim, Gyudo Park, Soohyeok Kang, and Simon S. Woo. S-vit: Sparse vision transformer for accurate face recognition. In *ACM SAC*, pages 1130–1138, 2023. [2](#)

- [25] Minchul Kim, Yiyang Su, Feng Liu, Anil Jain, and Xiaoming Liu. Keypoint relative position encoding for face recognition. In *IEEE/CVF Conference on Computer Vision and Pattern Recognition, CVPR 2024, Seattle, WA, USA, June 16-22, 2024*, pages 244–255. IEEE, 2024. [2](#), [4](#)
- [26] Alexander Kirillov, Eric Mintun, Nikhila Ravi, Hanzi Mao, Chloé Rolland, Laura Gustafson, Tete Xiao, Spencer Whitehead, Alexander C. Berg, Wan-Yen Lo, Piotr Dollár, and Ross B. Girshick. Segment anything. In *IEEE/CVF International Conference on Computer Vision, ICCV 2023, Paris, France, October 1-6, 2023*, pages 3992–4003. IEEE, 2023. [2](#)
- [27] Martin Knoche, Stefan Hörmann, and Gerhard Rigoll. Cross-quality LFW: A database for analyzing cross-resolution image face recognition in unconstrained environments. In *16th IEEE International Conference on Automatic Face and Gesture Recognition, FG 2021, Jodhpur, India, December 15-18, 2021*, pages 1–5. IEEE, 2021. [4](#), [5](#), [6](#)
- [28] Jan Niklas Kolf, Naser Damer, and Fadi Boutros. Grafiqs: Face image quality assessment using gradient magnitudes. In *2024 IEEE/CVF Conference on Computer Vision and Pattern Recognition Workshops (CVPRW)*, pages 1490–1499, 2024. [2](#), [5](#), [6](#)
- [29] Xialei Liu, Joost van de Weijer, and Andrew D. Bagdanov. Rankqa: Learning from rankings for no-reference image quality assessment. In *IEEE International Conference on Computer Vision, ICCV 2017, Venice, Italy, October 22-29, 2017*, pages 1040–1049. IEEE Computer Society, 2017. [1](#), [5](#), [6](#)
- [30] Ilya Loshchilov and Frank Hutter. Decoupled weight decay regularization. In *7th International Conference on Learning Representations, ICLR 2019, New Orleans, LA, USA, May 6-9, 2019*. OpenReview.net, 2019. [4](#)
- [31] Qiang Meng, Shichao Zhao, Zhida Huang, and Feng Zhou. Magface: A universal representation for face recognition and quality assessment. In *IEEE Conference on Computer Vision and Pattern Recognition, CVPR 2021, virtual, June 19-25, 2021*, pages 14225–14234. Computer Vision Foundation / IEEE, 2021. [1](#), [2](#), [4](#), [5](#), [6](#)
- [32] Anish Mittal, Anush Krishna Moorthy, and Alan Conrad Bovik. No-reference image quality assessment in the spatial domain. *IEEE Trans. Image Process.*, 21(12):4695–4708, 2012. [1](#), [5](#), [6](#)
- [33] Anish Mittal, Rajiv Soundararajan, and Alan C Bovik. Making a “completely blind” image quality analyzer. *IEEE SPL*, 20(3):209–212, 2012. [1](#)
- [34] Stylianos Moschoglou, Athanasios Papaioannou, Christos Sagonas, Jiankang Deng, Irene Kotsia, and Stefanos Zafeiriou. Agedb: The first manually collected, in-the-wild age database. In *2017 IEEE CVPRW, CVPR Workshops 2017, Honolulu, HI, USA, July 21-26, 2017*, pages 1997–2005. IEEE Computer Society, 2017. [4](#), [5](#), [6](#)
- [35] Xuan-Bac Nguyen, Duc Toan Bui, Chi Nhan Duong, Tien D. Bui, and Khoa Luu. Clusformer: A transformer based clustering approach to unsupervised large-scale face and visual landmark recognition. In *Proceedings of the IEEE/CVF Conference on Computer Vision and Pattern Recognition (CVPR)*, pages 10847–10856, 2021. [2](#)
- [36] Fu-Zhao Ou, Xingyu Chen, Ruixin Zhang, Yuge Huang, Shaixin Li, Jilin Li, Yong Li, Liujuan Cao, and Yuan-Gen Wang. SDD-FIQA: unsupervised face image quality assessment with similarity distribution distance. In *IEEE Conference on Computer Vision and Pattern Recognition, CVPR 2021, virtual, June 19-25, 2021*, pages 7670–7679. Computer Vision Foundation / IEEE, 2021. [1](#), [2](#), [5](#), [6](#)
- [37] Fu-Zhao Ou, Chongyi Li, Shiqi Wang, and Sam Kwong. Clib-fifa: Face image quality assessment with confidence calibration. In *Proceedings of the IEEE/CVF Conference on Computer Vision and Pattern Recognition (CVPR)*, pages 1694–1704, 2024. [4](#)
- [38] Lixiong Qin, Mei Wang, Chao Deng, Ke Wang, Xi Chen, Jiani Hu, and Weihong Deng. Swinface: A multi-task transformer for face recognition, expression recognition, age estimation and attribute estimation. *IEEE Trans. Circuits Syst. Video Technol.*, 34(4):2223–2234, 2024. [3](#), [4](#)
- [39] Torsten Schlett, Christian Rathgeb, Olaf Henniger, Javier Galbally, Julian Fierrez, and Christoph Busch. Face image quality assessment: A literature survey. *ACM Comput. Surv.*, 54(10s):210:1–210:49, 2022. [1](#)
- [40] Torsten Schlett, Christian Rathgeb, Juan E. Tapia, and Christoph Busch. Considerations on the evaluation of biometric quality assessment algorithms. *IEEE Trans. Biom. Behav. Identity Sci.*, 6(1):54–67, 2024. [4](#)
- [41] Soumyadip Sengupta, Jun-Cheng Chen, Carlos Domingo Castillo, Vishal M. Patel, Rama Chellappa, and David W. Jacobs. Frontal to profile face verification in the wild. In *2016 IEEE Winter Conference on Applications of Computer Vision, WACV 2016, Lake Placid, NY, USA, March 7-10, 2016*, pages 1–9. IEEE Computer Society, 2016. [4](#), [5](#), [6](#)
- [42] Yichun Shi and Anil K. Jain. Probabilistic face embeddings. In *2019 IEEE/CVF International Conference on Computer Vision, ICCV 2019, Seoul, Korea (South), October 27 - November 2, 2019*, pages 6901–6910. IEEE, 2019. [2](#), [5](#), [6](#)
- [43] Zhonglin Sun and Georgios Tzimiropoulos. Part-based face recognition with vision transformers. In *33rd British Machine Vision Conference 2022, BMVC 2022, London, UK, November 21-24, 2022*, page 611. BMVA Press, 2022. [2](#)
- [44] Philipp Terhörst, Jan Niklas Kolf, Naser Damer, Florian Kirchbuchner, and Arjan Kuijper. SER-FIQ: unsupervised estimation of face image quality based on stochastic embedding robustness. In *2020 IEEE/CVF Conference on Computer Vision and Pattern Recognition, CVPR 2020, Seattle, WA, USA, June 13-19, 2020*, pages 5650–5659. Computer Vision Foundation / IEEE, 2020. [2](#), [5](#), [6](#)
- [45] Philipp Terhörst, Jan Niklas Kolf, Naser Damer, Florian Kirchbuchner, and Arjan Kuijper. Face quality estimation and its correlation to demographic and non-demographic bias in face recognition. In *2020 IEEE Int. Joint Conf. on Biometrics (IJCB)*, pages 1–11. IEEE, 2020. [1](#)
- [46] Hao Wang, Yitong Wang, Zheng Zhou, Xing Ji, Dihong Gong, Jingchao Zhou, Zhifeng Li, and Wei Liu. Cosface: Large margin cosine loss for deep face recognition. In *2018 IEEE Conference on Computer Vision and Pattern Recognition, CVPR 2018, Salt Lake City, UT, USA, June 18-22, 2018*, pages 5265–5274. IEEE Computer Society, 2018. [3](#)

- [47] Joyce Yang, Patrick Grother, Mei Ngan, Kayee Hanaoka, and Austin Hom. Face Analysis Technology Evaluation (FATE) Part 11: Face Image Quality Vector Assessment – Specific Image Defect Detection. NIST Internal Report NIST IR 8485 DRAFT SUPPLEMENT, National Institute of Standards and Technology (NIST), Gaithersburg, MD, 2025. Image Group, Information Access Division, Information Technology Laboratory. This publication is available free of charge. [2](#)
- [48] Jinghan You, Shanglin Li, Yuanrui Sun, Jiangchuan Wei, Mingyu Guo, Chao Feng, and Jiao Ran. Lvface: Progressive cluster optimization for large vision models in face recognition, 2025. [3](#)
- [49] Hao Zhang, Feng Li, Shilong Liu, Lei Zhang, Hang Su, Jun Zhu, Lionel M. Ni, and Heung-Yeung Shum. DINO: DETR with improved denoising anchor boxes for end-to-end object detection. In *The Eleventh International Conference on Learning Representations, ICLR 2023, Kigali, Rwanda, May 1-5, 2023*. OpenReview.net, 2023. [2](#)
- [50] Kaipeng Zhang, Zhanpeng Zhang, Zhifeng Li, and Yu Qiao. Joint face detection and alignment using multitask cascaded convolutional networks. *IEEE Signal Process. Lett.*, 23(10):1499–1503, 2016. [4](#)
- [51] T. Zheng and W. Deng. Cross-pose lfw: A database for studying cross-pose face recognition in unconstrained environments. Technical Report 18-01, Beijing University of Posts and Telecommunications, 2018. [4](#), [5](#), [6](#)
- [52] Tianyue Zheng, Weihong Deng, and Jian Hu. Cross-age LFW: A database for studying cross-age face recognition in unconstrained environments. *CoRR*, abs/1708.08197, 2017. [4](#), [5](#), [6](#)
- [53] Yaoyao Zhong and Weihong Deng. Face transformer for recognition. *arXiv preprint arXiv:2103.14803*, 2021. [2](#)
- [54] Žiga Babnik, Peter Peer, and Vítomír Štruc. FaceQAN: Face image quality assessment through adversarial noise exploration. In *26th International Conference on Pattern Recognition (ICPR 2022)*, pages 748–754, Montreal, Canada, 2022. IEEE. [2](#)